A NUMERICAL AND EXPERIMENTAL INVESTIGATION ON SKIN CONDENSERS APPLIED TO HOUSEHOLD REFRIGERATORS

Elias G. Colombo, elias@polo.ufsc.br
Rodolfo S. Espíndola, rodolfo@polo.ufsc.br
Fernando T. Knabben, fernandok@polo.ufsc.br
Cláudio Melo, melo@polo.ufsc.br
POLO Laboratories, Department of Mechanical Engineering, Federal University of Santa Catarina
88040-970 - Florianópolis, SC, Brazil

Abstract. *In this study a numerical and experimental investigation on the performance of a skin condenser applied to a specific household refrigerator was carried out. To this end, a mathematical model which takes into account the heat transfer to both the environment and the refrigerated compartments was developed. The model uses as input data the internal and external air temperatures, refrigerant mass flow rate, pressure and temperature at the heat exchanger inlet and the condenser geometry to predict the condenser performance. Steady-state energy consumption tests – compressor running continuously with electric heaters being used to create artificial thermal load – were carried out under different operating conditions with the product inside a climate-controlled chamber. Tests were carried out at ambient temperatures of 25°C and 32°C, fresh-food compartment temperatures of 5°C and 10°C, freezer compartment temperatures of -20°C and -15°C and compressor speeds of 3000 rpm and 4500 rpm. Thermograms of the outer steel sheet temperature fields were recorded during the experiments. The model predictions were compared to a set of in-house experimental data with deviations within a ±2% error band. It was found that, on average, 68% of the condenser heat released rate is transferred to the environment while the remaining 32% is transferred to the refrigerated compartments. It was also found that the thermal conductivity of the tape used to attach the tubes plays an important role in determining the heat transfer rate, and the placement of the tubes in the region of the freezer walls should be avoided.*

Keywords*: skin condenser, household refrigerator, mathematical model, experimental validation*

1. NOMENCLATURE

A	cross-sectional area	(m^2)
d	tube outer diameter	(m)
h	enthalpy	(J/kg)
$\hbar$	heat transfer coefficient	($W/(m^2 \cdot K)$)
k	thermal conductivity	($W/(m \cdot K)$)
$\dot{m}$	mass flow rate	(kg/s)
N	compressor speed	(rpm)
P	pressure	(Pa)
$\dot{Q}$	heat transfer rate	(W)
R	thermal resistance	(K/W)
R''	thermal resistance per unit of area	($K/(W \cdot m^2)$)
t	thickness	(m)
T	temperature	(°C)
w	width	(m)

Subscripts

A	ambient A
ad	adhesive
amb	external ambient
avg	average
B	ambient B
c	air cavity
cond	condenser
ct	contact
f	fin
ff	fresh-food compartment
fz	freezer compartment
in	inlet
inf	infiltration

int	internal compartments
j	control volume index
m	generic ambient (A or B)
n	generic section (I, II, III, or IV)
os	outer metal sheet
out	outlet
pu	polyurethane
r	refrigerant
sd	side
t	tape
tb	tube

2. INTRODUCTION

Household refrigerators are composed of four main components: compressor, condenser, evaporator and expansion device. In the Brazilian market, most of the appliances are mounted with wire-and-tube condensers, due to their simplicity and low cost (Melo and Hermes, 2009). In the Asian market, however, skin condensers (also known as hot-wall condensers) are widely used. In this type of heat exchanger, the condenser tubes are attached to the inner surface of the refrigerator outer steel sheet by an adhesive tape (see Fig. 1), so the external walls act as fins and enhance the heat transfer to the environment. The main advantages are the possibility of reducing the manufacturing cost, the large heat exchange area and the refrigerator size reduction. On the other hand, part of the heat released by the condenser can infiltrate the refrigerated compartments and become an additional thermal load. Furthermore, if the tubes are not well attached to the outer sheet, a high thermal resistance is created and the heat rejection is reduced. Figure 2 shows an outer sheet thermogram of the refrigerator operating at an ambient temperature of 32°C. It can be noted that the highest temperatures of the outer metal sheet were in the area in direct contact with the condenser tubes. In addition, a bad contact between the tube and the outer sheet can be seen in the top of the Fig. 2, representing a manufacturing problem that reduces the system performance.

Despite the growing use of skin condensers, only a few reports on this topic can be found in the open literature. Rebora and Tagliafico (1998) carried out a study on the use of skin condensers and skin evaporators in horizontal freezers. In this case, the condenser and evaporator tubes are very close to each other and thus a large fraction of the heat released by the condenser can be by-passed to the evaporator, reducing the system performance. Bansal and Chin (2002) developed and validated a simulation model for hot-wall condensers used in domestic refrigerators. The authors disregarded the effect of the aluminum adhesive tape and considered that all the heat was rejected through the contact between the tube and the outer sheet, which was modeled as a fin. While recognizing that part of the heat is released to the refrigerated compartments, the mathematical model neglected any heat infiltration. They compared the model predictions to a set of experimental data and considered the results satisfactory, with deviations within a ±10% error band. Gupta and Gopal (2008) carried out some modifications to the model proposed by Bansal and Chin (2002), including the effect of the heat transfer through the aluminum tape, treating it as a fin. The model was validated with the experimental data of Bansal and Chin (2002) and a better agreement was observed, with deviations within a ±2% error band. In this context, the aim of the present study was to investigate the performance of skin condensers applied to household refrigeration systems. A mathematical model was developed considering the effect of the aluminum tape, the contact between the tubes and the outer sheet and the heat infiltration into the refrigerated compartments. In addition, tests were carried out with a frost-free domestic refrigerator in order to obtain experimental data to validate the model.

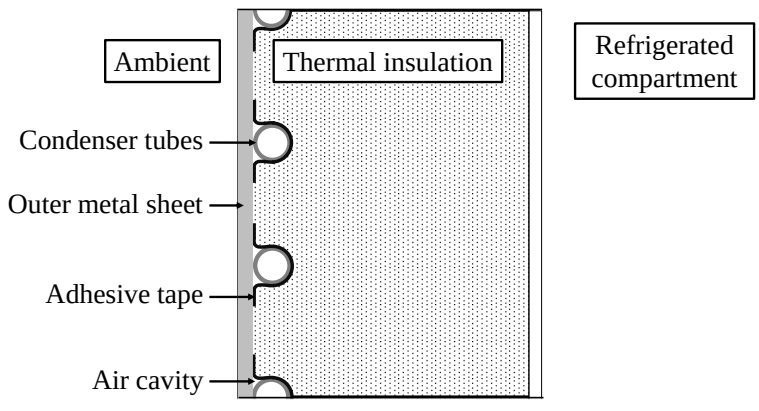

Figure 1. Skin condenser schematic view.

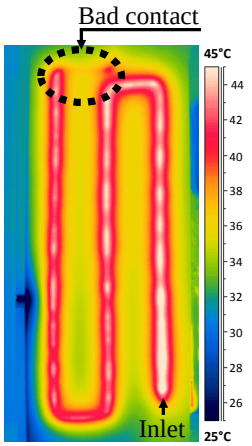

Figure 2. Outer sheet thermogram.

3. MATHEMATICAL MODEL

The first step is to discretize the condenser into small elements of length Δz. As shown in Fig. 3, each element consists of a portion of the condenser tube, the outer metal sheet, the aluminum adhesive tape and the thermal insulation. Since the arrangement of the condenser tubes is irregular, an average width (w_{avg}) was assumed for elements on the same wall (Bansal and Chin, 2002), defined by the wall surface area divided by the length of the tubes on the wall. Disregarding the pressure drop along the tubes and applying an energy balance in the element, the variation in the refrigerant enthalpy can be calculated through the following equation:

$$dh_j = h_{out,j} - h_{in,j} = -\frac{d\dot{Q}_j}{\dot{m}} \tag{1}$$

Understanding the condenser geometry is important to mapping the possible heat transfer paths and calculating the heat transferred on an elemental unit (dQ_j). As shown in Fig. 4, the refrigerant rejects heat to the condenser tube by internal forced convection. The heat can then be transferred either to the aluminum tape, to the outer metal sheet or to the air cavity. Part of the heat is then transferred from the outer metal sheet to the external ambient by natural convection and radiation, while part is conducted through the thermal insulation and infiltrates the cabinet.

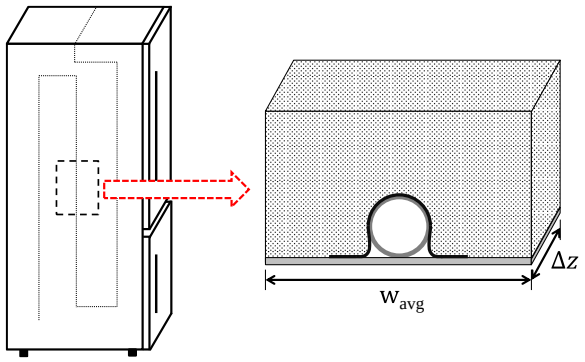

Figure 3. Condenser discretization.

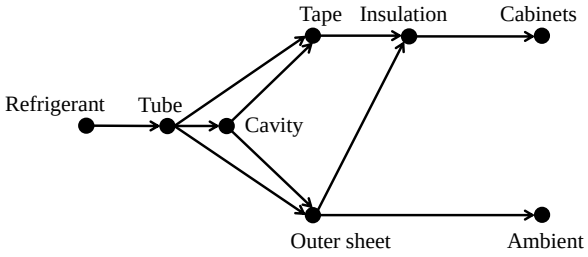

Figure 4. Heat transfer map.

The heat transfer to the external ambient air is governed by natural convection and radiation, as the outer steel sheet is thin and has a high thermal conductivity. On the other hand, the heat transfer to the refrigerated compartments is driven by conduction through the thermal insulation, which is thick and has a low thermal conductivity. Thus, the thermal resistances related to convection and radiation in the refrigerated compartments were neglected and the temperature of the internal walls was considered equal to that of the cold air.

Since the thermal conductivities of the aluminum tape and the outer steel sheet are high, a one-dimensional approach was adopted and both were treated as independent fins. Figure 5 shows a generic fin exposed to two ambient, A and B, with different temperatures and thermal resistances.

The ordinary differential equation (ODE) that describes the temperature profile of the generic fin can be obtained through an energy balance in the control volume shown in Fig. 5:

$$\frac{d^2T}{dx^2} - T\left(\frac{1}{R''_A} + \frac{1}{R''_B}\right)\frac{\Delta z}{k_f A_f} + \left(\frac{T_A}{R''_A} + \frac{T_B}{R''_B}\right)\frac{\Delta z}{k_f A_f} = 0 \tag{2}$$

Admitting that the terms R''_A, R''_B, T_A, T_B, Δz, k_f and A_f are constant along the x axis, the ODE can be solved analytically and the following equation for the temperature profile can be obtained:

$$T = C_1 e^{px} + C_2 e^{-px} + r/p^2 \tag{3}$$

where the constants C_1 and C_2 must be determined through appropriate boundary conditions, and the terms r and p^2 are given by the following equations:

$$r = \left(T_A/R''_A + T_B/R''_B\right)\left(k_f A_f\right)^{-1}\Delta z \tag{4}$$

$$p^2 = \left(1/R''_A + 1/R''_B\right)\left(k_f A_f\right)^{-1}\Delta z \tag{5}$$

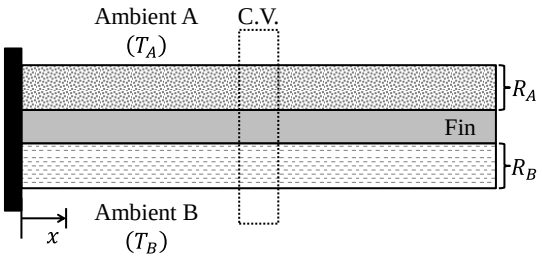

Figure 5. Generic fin.

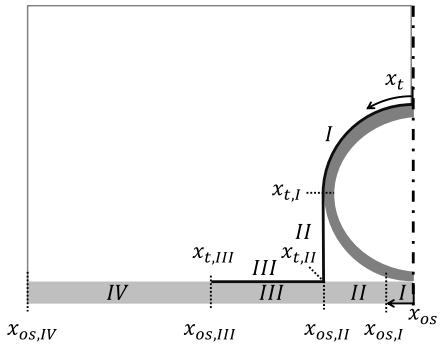

Figure 6. Sections of aluminum tape and outer sheet.

Equation (3) is generic and can be used to obtain the temperature profiles along the aluminum tape and the outer sheet, as long as the appropriate thermal resistances R''_A and R''_B, temperatures T_A and T_B and boundary conditions are taken into account for each case. The outer sheet and the aluminum tape were divided into sections as shown in Fig. 6. The first section of the aluminum tape is the region glued to the condenser tube. Due to the inherent variability of the manufacturing process, it was assumed that the tape is attached to half of the tube perimeter and follows a 90º angle in relation to the outer sheet. Thus, section II is the region in contact with the air cavity and section III represents the region attached to the outer sheet. Section I of the outer sheet represents the area of contact with the condenser tube. A very small contact of 0.5 mm was assumed. Section II is the region in contact with the air cavity. Section III represents the region in contact with the aluminum tape and section IV the region in contact with the thermal insulation. Table 1 groups the appropriate coefficients for each segment of the two fins.

As previously mentioned, the solution for the generic fin is valid only if the parameters R''_A, R''_B, T_A, T_B, k_f, A_f and Δz are constant along the fin length. As can be seen in Fig. 6, this is not the case in sections III of both the aluminum tape and outer sheet. In these cases, there is an interaction between the fins, so the generic solution cannot be used. The equation that represents the temperature profile of these sections can be obtained by solving the following system of differential equations:

$$\frac{d^2T_{os,III}(x_{os})}{dx_{os}^{\,2}} - T_{os,III}(x_{os})\left(\frac{1}{R''_{A,os,III}} + \frac{1}{R''_{B,os,III}}\right)\frac{\Delta z}{k_{os}A_{os}} + \left(\frac{T_{t,III}(x_t)}{R''_{A,os,III}} + \frac{T_{B,os,III}}{R''_{B,os,III}}\right)\frac{\Delta z}{k_{os}A_{os}} = 0 \tag{6}$$

$$\frac{d^2T_{t,III}(x_t)}{dx_t^{\,2}} - T_{t,III}(x_t)\left(\frac{1}{R''_{A,t,III}} + \frac{1}{R''_{B,t,III}}\right)\frac{\Delta z}{k_tA_t} + \left(\frac{T_{A,t,III}}{R''_{A,t,III}} + \frac{T_{os,III}(x_{os})}{R''_{B,t,III}}\right)\frac{\Delta z}{k_tA_t} = 0 \tag{7}$$

The analytical solutions for $T_{os,III}(x_{os})$ and $T_{t,III}(x_t)$ were obtained with the help of the mathematical software Maple, but were omitted since they are very extensive. Thus, 3 equations for the temperature profile of the aluminum tape sections and 4 equations for the outer sheet sections were determined. To complete the solution, 14 boundary conditions must be applied to determine the constants of each equation (see Tab. 2).

The temperature profiles must be integrated to calculate the heat transfer on the upper and lower sides of each section:

$$d\dot{Q}_{m,n} = \int_{x_1}^{x_2}\left[T(x) - T_{m,n}\right]R''^{\,-1}_{m,n}\Delta z dx \tag{8}$$

The heat transferred to the external ambient air is given by summing the heat transfer rates on the external surface of the outer sheet, as shown in Eq. (9). The heat transferred to the refrigerated compartments is given by summing the heat transfer rates from the upper side of the aluminum tape and the upper side of section IV in the outer sheet (Eq. 10). As the model considers only half of the elements due to symmetry, these values were multiplied by 2.

$$d\dot{Q}_{amb} = 2\left(d\dot{Q}_{B,os,I} + d\dot{Q}_{B,os,II} + d\dot{Q}_{B,os,III} + d\dot{Q}_{B,os,IV}\right) \tag{9}$$

$$d\dot{Q}_{\text{int}} = 2\left(d\dot{Q}_{A,t,I} + d\dot{Q}_{A,t,II} + d\dot{Q}_{A,t,III} + d\dot{Q}_{A,os,IV}\right) \tag{10}$$

The heat transferred by an elemental unit is given by the sum of the heat transferred to the external ambient air and the heat transferred to the refrigerated compartments:

$$d\dot{Q}_j = d\dot{Q}_{amb} + d\dot{Q}_{\text{int}} \tag{11}$$

It is important to mention that the problem is iterative, as the air cavity temperature, T_c, is still unknown. Thus, the problem is first solved with an estimate of T_c, and then its value is corrected through an energy balance for the air cavity. Assuming that the air cavity temperature is constant for an elemental unit:

$$d\dot{Q}_c + d\dot{Q}_{B,t,II} + d\dot{Q}_{A,os,II} = 0 \tag{12}$$

$$d\dot{Q}_c = 0.25\pi d\Delta z\left(T_r - T_c\right)\left(1/\hbar_r + t_{tb}/k_{tb} + 1/\hbar_c\right)^{-1} \tag{13}$$

where dQ_c is the heat transferred from the refrigerant to the air cavity, and $dQ_{B,t,II}$ and $dQ_{A,os,II}$ are the heat transfer rates exchanged with the air cavity in sections II in the aluminum tape and outer sheet, respectively.

Table 1. Temperatures and thermal resistances for each section.

Parameter	Aluminum tape			Outer metal sheet			
	I	II	III	I	II	III	IV
T_A	T_{int}	T_{int}	T_{int}	T_r	T_c	$T_{t,III}\left(x_t\right)$	T_{int}
T_B	T_r	T_c	$T_{os,III}\left(x_{os}\right)$	T_{amb}	T_{amb}	T_{amb}	T_{amb}
R''_A	t_{pu}/k_{pu}	t_{pu}/k_{pu}	t_{pu}/k_{pu}	$1/\hbar_r + R''_{ct}$	$1/\hbar_c$	R''_{ad}	t_{pu}/k_{pu}
R''_B	$1/\hbar_r + R''_{ad}$	$1/\hbar_c$	R''_{ad}	$1/\hbar_{amb}$	$1/\hbar_{amb}$	$1/\hbar_{amb}$	$1/\hbar_{amb}$

Table 2. Boundary conditions.

Aluminum tape		Outer sheet	
$x_t = 0$	$dT_{t,I}/dx_t = 0$	$x_{os} = 0$	$dT_{os,I}/dx_{os} = 0$
$x_t = x_{t,I}$	$dT_{t,I}/dx_t = dT_{t,II}/dx_t$ & $T_{t,I} = T_{t,II}$	$x_{os} = x_{os,I}$	$dT_{os,I}/dx_{os} = dT_{os,II}/dx_{os}$ & $T_{os,I} = T_{os,II}$
$x_t = x_{t,II}$	$dT_{t,II}/dx_t = dT_{t,III}/dx_t$ & $T_{t,II} = T_{t,III}$	$x_{os} = x_{os,II}$	$dT_{os,II}/dx_{os} = dT_{os,III}/dx_{os}$ & $T_{os,II} = T_{os,III}$
$x_t = x_{t,III}$	$dT_{t,III}/dx_t = 0$	$x_{os} = x_{os,III}$	$dT_{os,III}/dx_{os} = dT_{os,IV}/dx_{os}$ & $T_{os,III} = T_{os,IV}$
		$x_{os} = x_{os,IV}$	$dT_{os,IV}/dx_{os} = 0$

Finally, it is necessary to use appropriate correlations to calculate the heat transfer coefficients and compute the thermal resistances involved in the heat transfer process. For the external heat transfer, a combined heat transfer coefficient was assumed ($\hbar_{amb}$), given by the sum of the natural convection and radiation coefficients (Tagliafico and Tanda, 1997). The natural convection coefficient for the external ambient air was calculated by the correlations presented by Churchill and Usagi (1972) for heated vertical plates (side walls) and for horizontal heated upward facing plate (top wall). The forced convection coefficient for the refrigerant side was calculated according to the flow regime. For single-phase flow, Dittus and Boelter (1930) or Gnielinski (1976) correlations were used, depending on the Reynolds number. Two-phase flows were classified as annular for vertical tubes, and annular or stratified for horizontal tubes, according to the criteria presented by Chato (1962). For the air cavity, a constant value of 2 W/(m^2·K) was assumed due to its small volume and the low significance of its heat transfer (Gupta e Gopal, 2008). The thermal resistance of the tape adhesive was calculated as a conduction resistance with the data provided by the manufacturer. The adhesive is acrylic-based, with a 0.2 W/(m·K) thermal conductivity and a 40 μm thickness, resulting in thermal resistance of 0.0002 K/W. A constant value of 10^{-3} W/(m^2·K) was adopted for the thermal resistance of the contact between the condenser tube and the outer sheet (Nellis and Klein, 2008).

4. EXPERIMENTAL WORK

A 423-liter bottom-mount frost-free refrigerator, with a 120-liter freezer compartment placed below a 303-liter fresh-food compartment was used in the experiments. The system operates with 60 g of isobutane and is mounted with a finned-tube evaporator, a capillary tube-suction line internal heat exchanger and a reciprocating variable speed compressor. The condenser tubes are symmetrically distributed on the side walls (see Fig. 3). The side circuits are connected by a single pass in the top wall. It is important to note that the condenser tubes are located in both the fresh-food and freezer regions, so heat can infiltrate both compartments. The condenser has a total length of 10.7 m, with 5.0 m on each side wall and 0.7 m on the top wall. The main refrigerator characteristics are shown in Tab. 3.

Table 3. Refrigerator data.

Outer dimensions	Height	1.8 m
	Depth	0.8 m
	Width	0.7 m
Condenser tube	Material	Copper
	Outer diameter	4.0 mm
	Inner diameter	2.7 mm
Outer metal sheet	Material	Steel
	Thickness	0.5 mm
	Thermal conductivity	50 W/(m.K)
Adhesive tape	Material	Aluminum
	Width	50 mm
	Thickness	0.05 mm
	Thermal conductivity	170 W/(m.K)
Thermal insulation	Material	Polyurethane (PU)
	Fresh-food thickness	50 mm
	Freezer thickness	60 mm
	Thermal conductivity	0.0214 W/(m.K)

The condenser inlet and outlet were instrumented with T-type thermocouples (uncertainty of ±0.2°C) and absolute pressure transducers (uncertainty of ±0.01 bar). In addition, a Coriolis-type mass flow meter was installed at the compressor discharge (uncertainty of 0.1% of the readings). The condenser experimental capacity could thus be calculated as the product of the refrigerant mass flow rate and the enthalpy variation from the inlet (superheated vapor) to the outlet (subcooled liquid). The refrigerator was tested according to the steady-state methodology proposed by Hermes *et al.* (2013). In this methodology, electrical heaters are installed inside the refrigerated compartments to create an artificial thermal load and compensate for the excess in cooling capacity. The thermostat was deactivated and the compressor and fan ran continuously. A PID controller was used to modulate the heat released by the heaters and the compartment temperatures were controlled at predefined values. Sixteen tests were carried out at ambient temperatures of 25°C and 32°C, freezer compartment temperatures of -15°C and -20°C, fresh-food compartment temperatures of 5°C and 10 °C and compressor speeds of 3000 rpm and 4500 rpm. After reaching steady-state conditions, data were recorded for 1h and the value for each variable was taken as the average of the recorded data.

5. RESULTS AND DISCUSSIONS

The test results and the input data for the model are shown in Tab. 4. Figure 7 compares the experimental results for the model predictions. A reasonable agreement was observed and the model was capable of predicting the condenser capacity within a ±2% error band for all tests. Figure 8 shows the model estimates for the percentages of heat transfer released by the condenser. On average, 68% of the condenser heat transfer rate is directed to the external ambient while the remaining 32% infiltrates the refrigerated compartments. The average percentage of heat infiltration was 36% for tests 1 to 8 and 29% for tests 9 to 16, due to the higher ambient temperature in the first eight tests. The highest percentages for the heat infiltration were observed in tests 4 and 8 (40 and 42%, respectively), because of the higher ambient temperature and lower freezer temperature. Therefore, the placement of condenser tubes in the region of the freezer walls should be avoided.

Although the aforementioned percentages of heat infiltration might seem impressive, a few considerations must be made. Consider test 8, for example, where the heat infiltration through the side and top walls totalizes 50.9 W. Imagine now a situation where there are no condenser tubes attached to these walls. The thermal load in this case would be governed by the temperature difference between the external ambient air and the internal air, and no longer by the gradient between the condenser tube and the cold air. Through a simple heat transfer calculation, assuming only the thermal resistance related to conduction, a thermal load of 32.4 W can be estimated (see Eq. 14), which is not very different from the value obtained with the hot-wall condenser in place.

$$\dot{Q}_{\inf} = k_{pu} A_{sd,fz} l_{pu,fz}^{-1} \left(T_{amb} - T_{fz}\right) + k_{pu} A_{sd,ff} l_{pu,ff}^{-1} \left(T_{amb} - T_{ff}\right) + k_{pu} A_{top,ff} l_{pu,ff}^{-1} \left(T_{amb} - T_{ff}\right) \quad (14)$$

In order to investigate the model potential, a parametric analysis was carried out to check the impact of design parameters on the condenser performance, considering the following baseline case: ambient temperature of 32°C, fresh-food temperature of 5°C, freezer temperature of -18°C, refrigerant mass flow rate of 1.38 kg/h, and refrigerant temperature and pressure at the condenser inlet of 54°C and 6.3 bar, respectively.

Table 4. Experimental results.

Test #	T_{amb} [°C]	T_{ff} [°C]	T_{fz} [°C]	$T_{cond.in}$ [°C]	$T_{cond.out}$ [°C]	P_{cond} [bar]	$\dot{m}$ [kg/h]	N [rpm]
1	32.7	10.2	-14.3	64.1	41.9	7.07	1.62	4380
2	32.6	10.1	-14.8	57.0	41.6	6.63	1.45	3000
3	32.7	9.0	-19.8	60.3	39.8	6.57	1.40	4501
4	32.6	9.6	-19.9	53.4	43.1	6.09	1.24	3000
5	32.7	4.8	-14.9	64.3	41.7	7.03	1.61	4495
6	32.6	5.0	-14.8	57.4	42.0	6.65	1.48	2999
7	32.6	4.4	-19.6	60.8	40.0	6.61	1.44	4490
8	32.5	4.5	-19.7	54.1	41.4	6.20	1.30	2999
9	25.4	9.7	-14.9	53.6	31.6	5.86	1.43	4482
10	25.1	9.8	-15.0	46.7	31.3	5.51	1.31	2999
11	25.2	9.6	-20.0	52.3	32.3	5.62	1.40	4487
12	25.1	9.6	-20.0	46.3	33.5	5.32	1.30	3000
13	25.0	4.8	-15.2	55.0	33.3	5.94	1.54	4487
14	24.7	4.9	-15.3	47.4	32.3	5.50	1.40	3000
15	25.1	4.5	-19.9	51.9	31.9	5.51	1.37	4505
16	25.0	4.6	-20.0	45.6	31.6	5.26	1.26	2999

Figure 9 shows the condenser capacity and the percentage of heat infiltration as a function of the adhesive tape thermal conductivity. It was observed that for thermal conductivities lower than 100 W/(m·K) the capacity was strongly reduced and the heat infiltration increased. As the contact area between the condenser tubes and the outer sheet is very small, the adhesive tape plays an important role in the heat transfer because it acts as a fin, increasing the heat exchange area. Figure 10 shows the influence of the outer diameter of the condenser tube on the capacity. Although it seems contradictory, an increase in the tube diameter reduced the condenser performance. Since in this analysis the tape width was kept constant, an increase in the tube diameter led to a smaller contact area between the adhesive tape and the outer sheet, which reduced the heat rejection. Furthermore, as the mass flow rate was also kept constant, an increase in the tube cross-sectional area resulted in a reduction in the flow velocity and in the internal heat transfer coefficient.

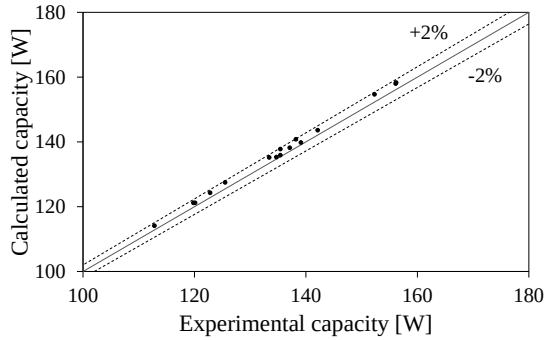

Figure 7. Model validation.

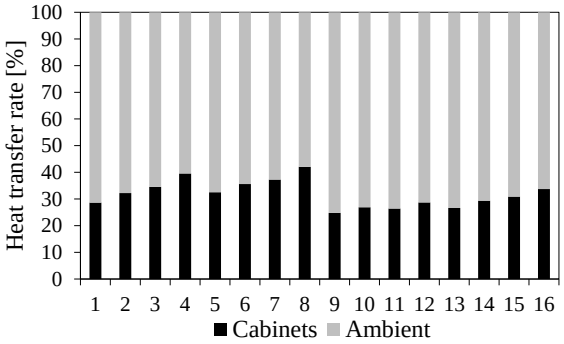

Figure 8. Heat transfer rates.

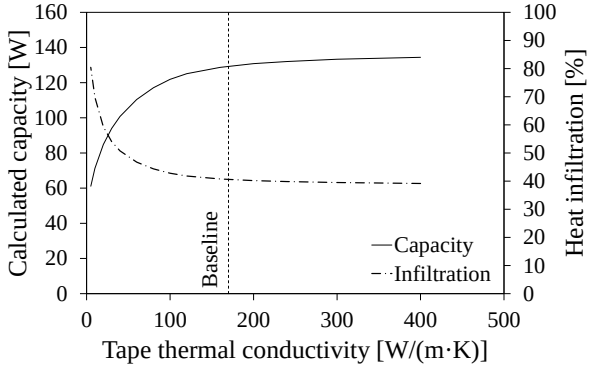

Figure 9. Capacity versus tape thermal conductivity.

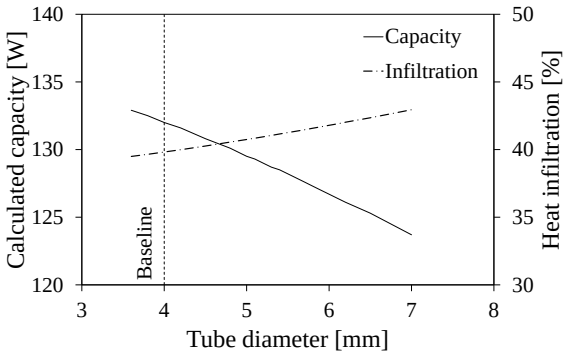

Figure 10. Capacity versus tube diameter.

The influence of the tape width was analyzed separately (see Fig. 11) and, as expected, the lower the tape width the lower the condenser capacity will be. Finally, the effect of the adhesive tape thickness on the heat transfer rate was evaluated and the results are shown in Fig. 12. Since the tape was modeled as a fin, an increase in its thickness resulted in a higher cross-sectional area and, consequently, a higher heat transfer rate.

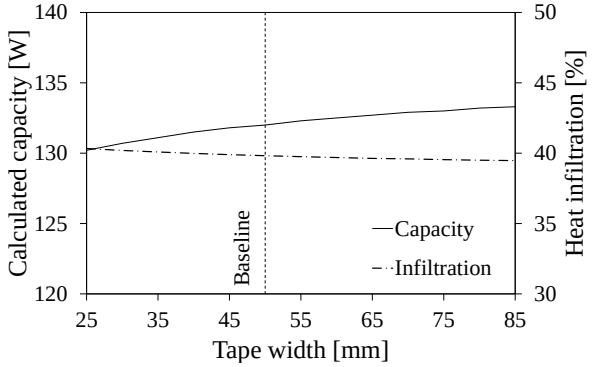

Figure 11. Capacity versus tape width.

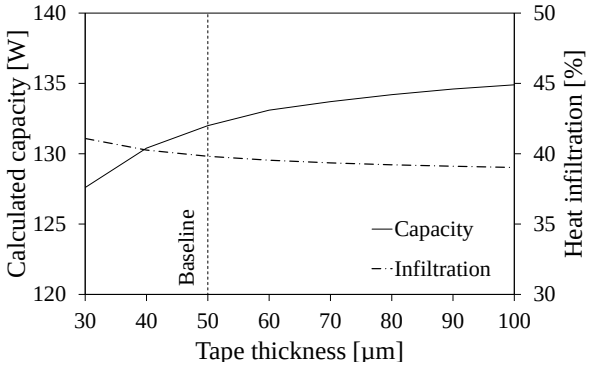

Figure 12. Capacity versus tape thickness.

5. CONCLUSIONS

This work involved an investigation of the characteristics and particularities of skin condensers applied to household refrigerators. A steady-state mathematical model for the condenser capacity prediction was put forward. The condenser heat transfer rate was calculated from the temperature profile of the aluminum tape and the outer metal sheet, which were both treated as one-dimensional fins. The model considered heat rejection to both the external ambient air and the refrigerated compartments. Sixteen tests were carried out with a bottom-mount frost-free refrigerator, under different operating conditions. The model predictions were compared to the experimental data with deviations within a ±2% error band. It was noted that, on average, 68% of the condenser heat transfer rate is directed to the ambient air while the remaining 32% is transferred to the refrigerated compartments. In addition, a parametric analysis showed that the thermal conductivity of the tape plays an important role in determining the heat transfer rate. It was also observed that the tubes should not be located in the region of the freezer walls, as the temperature gradient between the condenser tubes and the freezer is high, increasing the heat infiltration rate.

6. ACKNOWLEDGEMENTS

This study was made possible through the financial investment from the EMBRAPII Program (POLO/UFSC EMBRAPII Unit - Emerging Technologies in Cooling and Thermophysics). The authors thank Embraco S.A. and Whirlpool S.A. for financial and technical support.

7. REFERENCES

Bansal, P. K. and Chin, T. C, 2002. "Design and modeling of hot-wall condensers in domestic refrigerators". Applied Thermal Engineering, Vol. 22, No. 14, pp. 1601–1617.

Chato, J. C., 1962. "Laminar condensation inside horizontal and inclined tubes". ASHRAE Journal, Vol. 4, No. 2, pp. 52–60.

Churchill, S. W. and Usagi, R., 1972. "A General Expression for the Correlation of Mass Transfer Rates and Other Phenomena". AIChE Journal, Vol. 18, No. 6, pp. 1121–1128.

Dittus, F. W. and Boelter, L. M. K., 1930. "Heat Transfer in Automobile Radiators of the Tubular Type". Publication in Engineering, Vol. 2, p. 443.

Gnielinski, V., 1976. "New equations for heat and mass transfer in turbulent pipe and channel flow". International Journal of Chemical Engineering, Vol. 16, No. 2, pp. 359–387.

Gupta, J. K. and Gopal, M. R., 2008. "Modeling of hot-wall condensers for domestic refrigerators". International Journal of Refrigeration, Vol. 31, No. 6, pp. 979–988.

Hermes, C. J. L., Melo, C. and Knabben, F. T., 2013. "Alternative test method to assess the energy performance of frost-free refrigerating appliances". Applied Thermal Engineering, Vol. 50, No. 1, pp. 1029–1034.

Melo, C. and Hermes, C. J. L., 2009. "A heat transfer correlation for natural draft wire-and-tube condensers". International Journal of Refrigeration, Vol. 32, No. 3, pp. 546–555.

Nellis, G. and Klein, S., 2008. Heat Transfer. Cambridge University Press, New York.

Rebora, A. and Tagliafico, L. A., 1998. "Thermal performance analysis for hot-wall condenser and evaporator configurations in refrigeration appliances". International Journal of Refrigeration, Vol. 21, No. 6, pp. 490–502.

Tagliafico, L. A. and Tanda, D. W., 1997. "Radiation and natural convection heat transfer from wire-and-tube heat exchangers in refrigeration appliances". International Journal of Refrigeration, Vol. 20, No. 7, pp. 461–469.

8. RESPONSIBILITY NOTICE

The authors are the only responsible for the printed material included in this paper.